J Therm Anal Calorim (2017) 127:1655–1661
DOI 10.1007/s10973-016-5632-2

# Thermal behavior of quinoxaline 1,4-di-*N*-oxide derivatives

**Elena Lizarraga**[1] · **Camino Zabaleta**[1] · **Juan A. Palop**[1]

Received: 17 December 2015 / Accepted: 12 June 2016 / Published online: 5 July 2016


**Abstract** The thermal hazard of a series of quinoxaline 1,4-di-*N*-oxide derivatives, designed to act as prodrugs, whose chemical structure undergoes a very rapid decomposition, has been evaluated. The fusion and thermal decomposition of the compounds have been studied by thermogravimetry, differential scanning calorimetry, and mass spectrometry (MS-DIP). The results obtained indicate that the decomposition process from the loss of one of the oxygens linked to a nitrogen of the quinoxaline involves the release of a large quantity of vapor in a very small time interval. The enthalpy is higher than 300 J $g^{-1}$; in some cases, it is around 1000 J $g^{-1}$.

**Keywords** Thermal analysis · Decomposition · Thermogravimetry · Thermal hazard · Explosive

## Introduction

To be aware of the hazards associated with chemical substances, whether these substances are involved in a given process or simply transported or stored, is essential so that preventative measures can be adopted. Estimating the degree of hazard of a substance due to its reactivity is very complex because both the characteristics of the substance itself and the conditions in which the substance can react with another one exert their influence [1, 2].

✉ Elena Lizarraga
elizarraga@unav.es

[1] Department of Organic and Pharmaceutical Chemistry, Faculty of Pharmacy, University of Navarra, Irunlarrea 1, 31008 Pamplona, Spain

Many accidents are caused by thermal runaway reactions. Thermal runaway occurs when the reaction rate increases due to an increase in temperature [3]. Incidents can occur during preparation, manufacturing process, storage, transport, or usage in industrial transformation. If accidental contamination and thermal exposure are not prevented, runaway reactions leading to an accident could be triggered during any of these stages [4].

Runaway reactions often involve a high exothermic peak that could induce a thermal accident and damage the process equipment and the surroundings [5]. The phenomena derived from dangerous reactivity are diverse: brusque heating of the mass, uncontrolled boiling, projections, and explosions of chemical reactors due to overpressure associated with rapid releases of gas, explosive decompositions, spontaneous combustion, etc. Normally, these phenomena are due to exothermic reactions, with releases of energy that become uncontrollable and provoke accidents. The explosion potential or ignition of a substance can be estimated based on thermal data [6–8].

Researches on intermediate hazardous compounds within the field of organic synthesis can represent a vital and additional area of application for the DSC technician. Differential scanning calorimetry and thermogravimetry (TG) have been used as part of the strategy for evaluating the thermal hazard of synthetic intermediates and pharmaceutical products, defining thermal hazard as the uncontrolled and/or unexpected release of energy which can cause the release of fire, explosion, and environmental problems [9, 10]. Caution should be exercised when synthesizing and isolating products that show this hazardous behavior [11].

The most important characteristics of thermal hazards from the studies of calorimetry stressed the exothermic onset temperature, heat of reaction, maximum temperature,

adiabatic temperature rise, maximum pressure, pressure rising rate, maximum self-heat rate, and time to maximum rate [12, 13].

A material that exhibits large exothermal decomposition with large negative enthalpy changes (energy $> 300$ J $g^{-1}$) at low temperatures, below 150 °C, in a DSC curve, can generate a large volume of decomposition gas products with the resultant risk of explosion. A substance was classified as highly hazardous substance as the exothermic reaction heat was higher than 250 J $g^{-1}$ [14, 15].

In cases where this type of potentially explosive behavior is detected, the appearance of endothermic processes, as fusions or desolvations, preceding decomposition stabilizes the compounds. However, if the compounds studied melt and decompose jointly, the protective effect is relatively small because the sample dissolves in its own decomposition products or in the part of itself that is melted [9].

It has been observed that the most important characteristic of the thermal profile of some compounds, that are representative of pharmaceuticals in the developing stage, corresponds to thermogravimetric curves which reflect a large release of degradation vapors within a narrow temperature interval, graphically expressed in the TG curve as a very large drop and in the DTG curve, as a very sharp peak [16].

The potential thermal hazard of some quinoxaline derivatives has been assessed. The quinoxaline scaffold is present in several compounds that show very interesting biological properties, and there is active interest in their research concerning medicinal chemistry. More importantly, its oxidized form, with quinoxaline 1,4-di-*N*-oxide (QDO) scaffold, greatly increases the biological properties of the structure [17]. In fact, the QDO derivatives are known as being anti-infective agents and they are cytotoxic against hypoxic cells present in solid tumors, with anti-Candida, anti-protozoal, and mutagenic properties. In addition, our research team has investigated and developed a large number of quinoxaline 1,4-di-*N*-oxide derivatives exhibiting a diverse range of therapeutic properties [18–22].

Because the synthesis of several benzoheterocycles (as quinoxalines and quinazolines) containing nitro, amino, and *N*-oxide substituents has been also investigated for their potential application as explosive molecules [23], the potential thermal hazard of several quinoxaline 1,4-di-*N*-oxide derivatives, designed to act as prodrugs, has been evaluated.

## Experimental

### Materials

Seven new quinoxaline 1,4-di-*N*-oxide derivatives have been studied. The structures of the compounds are shown in Table 1, and they have been provided by the Organic and Pharmaceutical Synthesis Unit of the University of Navarra.

Each product is accompanied by identification assays which include: elemental analysis, infrared spectroscopy, 1H-NMR spectroscopy, HPLC, thermomicroscopy, mass spectrometry, and possible additional observations related to the solubility of the product, and alteration of the properties with light or heat. The compounds achieve a high grade of purity because they were prepared for carrying out biological assays.

### Equipment and procedures

#### *Thermal analysis: thermogravimetry and differential scanning calorimetry*

The *calorimetric studies* are carried out with a PerkinElmer DSC-7 which was calibrated with indium and zinc (provided by PerkinElmer and fabricated according to guideline ISO35) at 10 °C $min^{-1}$ and a nitrogen flow of 40 mL $min^{-1}$. The gases connected to the equipment are nitrogen and air with a purity of 99.999 %.

First of all, preliminary calorimetric analysis has been performed to determine the stability of each compound in the range of fusion temperatures, studying possible desolvations, solid–solid transitions, fusion, purity, etc. This facilitates the selection of those compounds which are stable, pure, and do not present polymorphism.

Calorimetric analyses are performed in aluminum capsules for volatiles of 10 μL, at heating rates of 20, 10, and 5 °C $min^{-1}$, using a sample of approximately 3 mg, to find the $T_{onset}$, $T_{max}$, and the enthalpy of fusion, $\Delta H_f$. Five

**Table 1** Quinoxaline 1,4-di-*N*-oxide derivatives

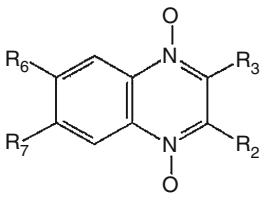


| Reference | R2 | R3 | R6 | R7 |
|---|---|---|---|---|
| *D-001* | $-NH_2$ | –CN | –H | –H |
| *D-002* | $-NH_2$ | –CN | –Cl | –H |
| *D-003* | $-NH(CH_2)_3N(CH_3)_2$ | –CN | –H | –H |
| *D-004* | $-NH_2$ | –CN | –Cl | –F |
| *D-005* | $-NH_2$ | –CN | $-OCH_3$ | –H |
| *D-006* | $-CH_3$ | –H | –Cl | –Cl |
| *D-007* | $-NHCONH(CH_2)_2N(CH_3)_2$ | –CN | –H | –H |

calorimetric analyses are carried out. The mean, standard deviation, and variation coefficient are calculated.

*Thermogravimetric studies* were carried out with a PerkinElmer TGA-7. The thermobalance was calibrated with alumel and nickel at 10 °C $min^{-1}$. The calibration of the oven temperatures was carried out automatically. Mass calibration was realized with a certified mass of 100 mg (ASTM E617).

Thermogravimetric analyses are performed under air atmosphere with a gas flow of 40 mL $min^{-1}$, at 20, 10, and 5 °C $min^{-1}$, using a mass sample of approximately 3 mg. The $T_{initial}$, $T_{onset}$, and $T_{max}$, as well as any associated mass loss, are calculated. Five thermogravimetric analyses are carried out to calculate the mean, standard deviation, and variation coefficient. The mass losses and heat responses of the changes in the sample were measured in the temperature range from 100 to 450 °C.

### *Mass spectral measurements and instrument*

The mass spectra (MS-DIP) have been carried out using a Agilent 5973A with electron impact ionization at 70 eV. The samples were introduced by means of direct insert probe (DIP). The instrument was calibrated using perfluorotributylamine as standard material.

For the purpose of determining the composition of the degradation vapors, they have been collected at the gas outlet of the thermobalance oven by means of solid-phase extraction, forcing the vapors through a minicolumn C18 previously conditioned with methanol. The substances retained in the column are extracted with 1 mL of methanol and then identified by mass spectrometry.

## Results and discussion

### Calorimetric data

In the thermal curve obtained at 2 °C $min^{-1}$ from compound *D-001* (Fig. 1), an exothermic peak is observed with a $T_{onset}$ of degradation of 231.5 °C, $T_{peak}$ = 234.4 °C, and $\Delta H$ associated with the process of 1013.3 J $g^{-1}$.

The degradation exotherm corresponds to the joint process of fusion and degradation of the compound. The release of vapors is so large that using higher heating rates favors an almost instantaneous release of vapors when the process temperature is reached. Therefore, a low heating rate was selected for this study.

Figure 2 represents the fusion/degradation processes of compound *D-003* reflected in the exothermic peak that appears in the thermal curves obtained at different heating rates (20, 10, and 5 °C $min^{-1}$). The temperatures and

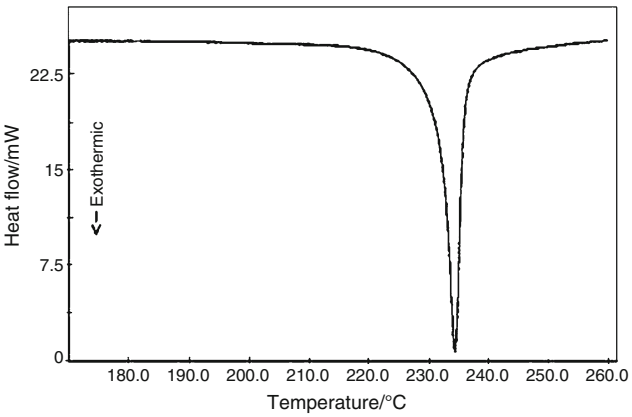


**Fig. 1** DSC curve of D-001 compound at 2 °C $min^{-1}$

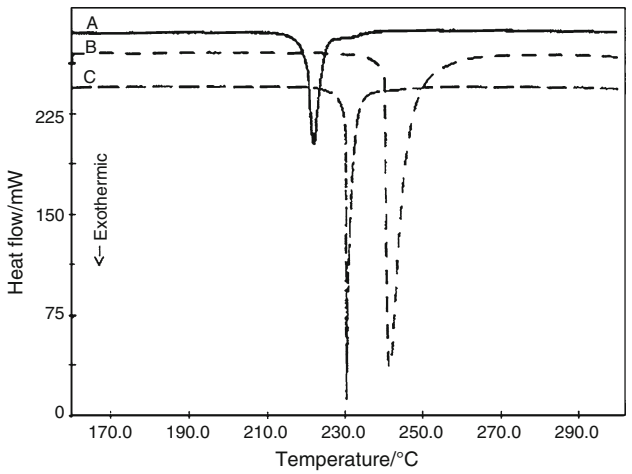


**Fig. 2** DSC curves of D-003 compound at (*a*) 5 °C $min^{-1}$; (*b*) 20 °C $min^{-1}$; (*c*) 10 °C $min^{-1}$

**Table 2** Temperatures (°C) and $\Delta H$ (J $g^{-1}$) of fusion/degradation process (DSC)

| Fusion/degradation process (DSC) | | | | | | |
|---|---|---|---|---|---|---|
| | $T_{onset}$/°C | SD | $T_{max}$/°C | SD | $\Delta H$/J $g^{-1}$ | SD |
| *D-001* | | | | | | |
| 2 °C $min^{-1}$ | 231.5 | – | 234.4 | – | 1013.3 | – |
| *D-003* | | | | | | |
| 5 °C $min^{-1}$ | 219.9 | – | 222.0 | – | 1141.1 | – |
| 10 °C $min^{-1}$ | 230.5 | 1.0 | 230.9 | 1.0 | 1037.1 | 13.9 |
| 20 °C $min^{-1}$ | 236.4 | 5.3 | 237.6 | 5.3 | 1167.8 | 17.2 |
| *D-004* | | | | | | |
| 5 °C $min^{-1}$ | 196.7 | – | 209.4 | – | 1167.8 | – |
| 20 °C $min^{-1}$ | 237.0 | 2.5 | 240.0 | 2.1 | 1096.0 | 21.1 |
| *D-008* | | | | | | |
| 5 °C $min^{-1}$ | 184.9 | 0.6 | 185.3 | 0.6 | 1120.9 | 28.3 |
| 10 °C $min^{-1}$ | 190.9 | 2.0 | 191.4 | 1.8 | 1043.1 | 16.2 |

*SD* standard deviation

– Single analysis

enthalpies associated with the exothermic peak process are shown in Table 2.

Compounds *D-004 and D-008* present the same behavior; a very sharp exothermic peak corresponding to the fusion and decomposition of each compound is observed. The $\Delta H$ associated with the process is not modified with the heating rate, being greater than 1000 J $g^{-1}$ in each case (Table 2).

Heat can be accumulated in the reaction system to cause temperature to be increased. When the system temperature reaches the apparent exothermic onset temperature ($T_{onset}$), this reaction system gradually becomes unstable and a self-reactive reaction is activated. If the temperature reached a specific threshold value, this reagent system would inevitably trigger a runaway reaction or explosion [7].

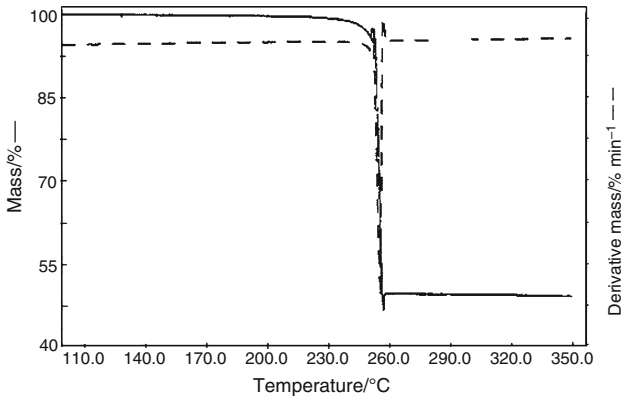


**Fig. 3** TG (*straight line*) and DTG (*dash line*) curves of D-001 compound at 10 °C $min^{-1}$

## Thermogravimetric data

The influence that the heating rate has on the thermal behavior of the compounds has shown that in each case, high rates favor explosive behavior [24]. Compounds D-001, D-004, and D-006 showed this behavior in all the assay conditions that were used. However, compounds D-002, D-003, D-005, and D-007 modify their thermal behavior with the heating rate, showing explosive behavior only when rapid heating rates are used (10 and/or 20 °C $min^{-1}$).

### *Compounds D-001, D-004, and D-006*

In the TG curve of compound *D-001* (Fig. 3), at 10 °C $min^{-1}$, two transitions can be distinguished: In the first one, there is a very small gradual mass loss. In the second transition, which corresponds with the degradation process, there is a large mass loss (47.88 %) which is clearly observed in the DTG curve by means of an

**Table 3** Temperatures of degradation process and degradation rates (TG)

| | Temperature | | % Degradation | | |
|---|---|---|---|---|---|
| | $T_{max}$/°C | $T_{final}$/°C | % ($T_{max}$) | $w_\infty$/% | $v_{max}$/% $min^{-1}$ |
| *D-001* | | | | | |
| 10 °C $min^{-1}$ | 254.5 | 256.8 | 28.95 | 47.88 | 255.49 |
| SD | 0.8 | 0.8 | 0.83 | 2.66 | 32.47 |
| 5 °C $min^{-1}$ | 255.3 | 257.4 | 28.67 | 52.88 | 137.43 |
| SD | 1.6 | 1.1 | 1.20 | 2.27 | 0.94 |
| 20 °C $min^{-1}$ | 262.0 | 264.8 | 29.87 | 44.08 | 556.88 |
| SD | 1.4 | 1.1 | 0.88 | 2.51 | 44.26 |
| *D-002* | | | | | |
| 10 °C $min^{-1}$ | 260.9 | 262.7 | 25.25 | 64.30 | 104.81 |
| SD | 2.6 | 3.2 | 1.72 | 1.72 | 19.19 |
| *D-003* | | | | | |
| 10 °C $min^{-1}$ | 245.8 | 253.0 | 11.56 | 78.67 | 39.91 |
| SD | 0.2 | 6.3 | 0.92 | 1.55 | 8.35 |
| 20 °C $min^{-1}$ | 255.6 | 259.4 | 14.51 | 73.12 | 146.82 |
| SD | 1.1 | 0.5 | 1.21 | 2.64 | 10.87 |
| *D-005* | | | | | |
| 10 °C $min^{-1}$ | 286.7 | 290.87 | 60.62 | 60.62 | 50.07 |
| SD | 0.2 | 6.3 | 0.92 | 1.55 | 8.35 |

% ($T_{max}$): mass loss at $T_{max}$; *SD* standard deviation

$w_\infty$ residue at $T_{final}$

**Table 4** Mass spectra with the most important fragments of quinoxaline 1,4-di-*N*-oxides derivatives and decomposition vapors

| Relative abundance/% | | | | |
|---|---|---|---|---|
| | Molecular ion | Loss of oxygen of *N*-oxide (position 1) | Loss of oxygen of *N*-oxide (position 4) | Loss of HCN |
| *D-001* | *100.00 (m/z = 202.15)* | *46.78 (m/z = 186.15)* | *8.66 (m/z = 170.15)* | *2.89 (m/z = 144.15)* |
| Vapors of D-001 | 6.77 | 100.00 | 53.86 | – |
| *D-002* | *100.00 (m/z = 236.00)* | *61.79 (m/z = 220.00)* | *25.47 (m/z = 204.00)* | *17.30 (m/z = 178.00)* |
| Vapors of D-002 | 3.56 | 100.00 | 79.20 | 47.87 |
| *D-004* | *59.42 (m/z = 254.00)* | *100.00 (m/z = 238.00)* | *23.87 (m/z = 222.00)* | *14.45 (m/z = 196.00)* |
| Vapors of D-004 | 2.06 | 100.00 | 45.73 | 25.73 |
| *D-005* | *100.00 (m/z = 266.00)* | *40.60 (m/z = 250.00)* | *13.45 (m/z = 234.00)* | *25.11 (m/z = 235[a])* |
| Vapors of D-005 | 1.48 | 100.00 | 76.09 | 74.91 |

[a] Loss of $CH_3$ from m/z = 250.00

Italic values indicate relative abundances/% of ions at a value of m/z (mass number/charge number)

extremely sharp peak (252–256.8 °C). The high rate value corresponding to loss of mass at maximum temperature ($v_{max}$ = 255.49 % $min^{-1}$) is clearly superior to that obtained for other thermal behaviors (20–60 % $min^{-1}$). The temperatures and percentages that are characteristics of this transition are shown in Table 3.

The thermal curve and data obtained at 5 and at 20 °C $min^{-1}$ show the same thermal occurrence (see Table 3). The high $v_{max}$ value obtained in the analysis at 20 °C $min^{-1}$ (556.88 % $min^{-1}$) confirms that high heating rates favor this explosive procedure.

The same behavior was observed in compounds *D-004* and *D-006*. The DTG curve of compound D-004 shows, in the second transition (from 289.3 to 293.3 °C, with a mass loss of 30.91 and 50.74 % of final residue), a $v_{max}$ of 129.81 % $min^{-1}$, which corresponds to a explosive behavior.

The second stage (231.1–233.2 °C) of the thermal curve of compound D-006 shows a mass loss of 39.84 %, with a residue of 50.96 % at this temperature. The $v_{max}$ reached in the second transition is 406.75 % $min^{-1}$, thereby showing that the compound presents hazardous thermal behavior.

In the majority of the cases, the *mass spectrum* of the vapors that were collected at the TG gas outlet corresponds to a degradation product resulting from the loss of an oxygen of the *N*-oxide group from the structure of the compounds and which is eliminated at a fast rate. Table 4 shows the most important fragments of the mass spectra of D-001 and D-004; it also shows the spectrum obtained from the decomposition vapors.

### *Compounds D-002, D-003, D-005, and D-007*

These compounds modified their thermal behavior with the assay conditions used.

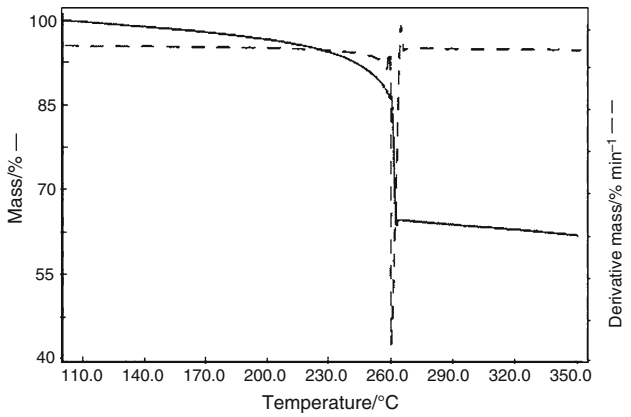


**Fig. 4** TG (*straight line*) and DTG (*dash line*) curves of D-002 compound at 10 °C $min^{-1}$

The TG curve of compound *D-002* at 10 °C $min^{-1}$ (Fig. 4) shows two transitions.

While the first transition occurs with a small mass loss, the second transition (from 260.9 to 262.7 °C, with a mass loss of 64.30 %) occurs with a rapid mass loss (104.81 % $min^{-1}$). This is represented as a very sharp peak on the DTG curve.

It was observed that, at 5 °C $min^{-1}$, the compound did not present this thermal behavior ($v_{max}$ was 24.74 % $min^{-1}$). However, at 20 °C $min^{-1}$, the $v_{max}$ was 218.38 % $min^{-1}$. The data show the large influence of the heating rate on the decomposition behavior of D-002, due to the fact that at high rates, the temperature of the sample can be higher than the temperature marked by the program used by research team, with this slight elevation of temperature triggering the hazardous behavior.

The variation observed in the relative abundance of the most important fragments of the mass spectrum of D-002 and in their vapors has been studied; results are shown in Table 4. By analyzing the results, it is evident that in the

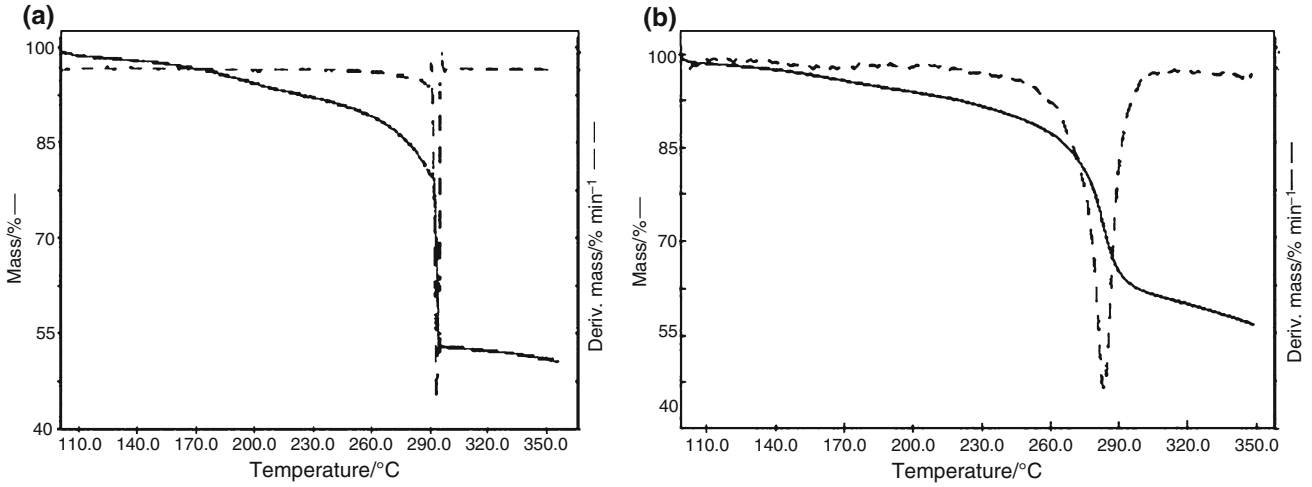


**Fig. 5** TG (*straight line*) and DTG (*dash line*) curves of D-005 compound at (**a**) 20 °C $min^{-1}$ and (**b**) 5 °C $min^{-1}$

degradation of compound D-002, the most abundant degradation product produced was as result of a loss of one of the *N*-oxides which was released quickly, almost instantaneously.

The experimental data have shown that the $v_{max}$ of the second transition in the TG curve, at 10 °C $min^{-1}$, of compound *D-003* is 39.91 % $min^{-1}$ and does not present explosive behavior as it does at 20 °C $min^{-1}$ when the $v_{max}$ increases considerably up to 146.82 % $min^{-1}$. Table 3 shows the temperatures that are characteristic of the second transition.

The mass spectrum obtained after collecting vapors shows a fragment with m/z = 204.00 which corresponds to the fragment 2-amino-3-cyano-7-chloroquinoxaline; therefore, it can be assumed that the aliphatic chain was lost in the thermal decomposition.

The second transition of TG curve of the compound *D-005* has been studied at 5, 10, and 20 °C $min^{-1}$. At 5 °C $min^{-1}$ and at 10 °C $min^{-1}$ ($v_{max}$ 7.81 % $min^{-1}$ and 50.07 % $min^{-1}$, respectively), and at 20 °C $min^{-1}$, the $v_{max}$ becomes 230.56 % $min^{-1}$ (Table 3). In this compound, the effect of the heating rate is very marked: At 5 °C $min^{-1}$, the degradation rate is slow, at 10 °C $min^{-1}$, this process is fairly fast, and at 20 °C $min^{-1}$, it changes to explosive rate (Fig. 5).

The mass spectrum of the vapors identified the degradation product obtained from the loss of an oxygen of the *N*-oxide group of compound D-005 (Table 4).

The second transition of compound *D-007* at 10 °C $min^{-1}$ began at approximately 200 °C and finalizes at 220.4 °C, with an 86.69 % sample residue. The $v_{max}$ is around 16 % $min^{-1}$. If the assay is carried out at 20 °C $min^{-1}$, it can be observed that the $v_{max}$ reaches 253.30 % $min^{-1}$ and then an explosive behavior began. This compound, which present the group –NHCONH($CH_2$)$N(CH_3)_2$ (a quite labile center), shows the lowest $T_{initial}$ value of all compounds.

## Conclusions

The thermal behavioral parameters for a series of quinoxaline 1,4-di-*N*-oxide derivatives whose chemical structure undergoes a very rapid decomposition have been identified in order to evaluate their possible hazardous behavior.

The results from the TG and DSC curves indicate that the decomposing process, characterized by the loss of one of the oxygens linked to the nitrogen of the quinoxaline, appears to present high activation energy, but once the process is initiated, due to an increase in the temperature, it feeds itself because it is quite exothermic, producing an aggressive emission of vapors and a large release of energy in a narrow temperature interval, that is not usual in the degradation behavior of organic compounds.

The study on thermal behavior in the fusion process carried out using DSC showed that the quinoxaline 1,4-di-*N*-oxide derivatives studied undergo fusion with an aggressive exothermal decomposition that produces a large release of energy. In addition, the enthalpy changes associated with the process (energy released in the decomposition) are extremely high, greater than 300 J $g^{-1}$, and in some cases around 1000 J $g^{-1}$. The thermal behavior is produced upon modifying the assay conditions.

It can be concluded that the quinoxaline 1,4-di-*N*-oxide derivatives studied can be classified as "thermal hazardous compounds" and preventive measures could be adopted when synthesizing and isolating them. However, the thermogravimetric data indicate that the beginning of the thermal decomposition is greater than 200 °C, thereby being able to eliminate a high risk of explosion of these compounds.

## References


1. Bestraten M. Nota Técnica de Prevención, NTP 302 "Reactividad e inestabilidad química: análisis termodinámico preliminar" Ministerio de Trabajo y Asuntos Sociales. España. 1999.
2. Calvet S. Nota Técnica de Prevención, NTP 527 "Reacciones químicas exotérmicas (I): factores de riesgo y prevención" Ministerio de Trabajo y Asuntos Sociales. España. 1999.
3. You ML, Tseng JM, Liu MY, Shu CM. Runaway reaction of lauroyl peroxide with nitric acid by DSC. J Therm Anal Calorim. 2010;102:535–9.
4. Hsueh KH, Chen WC, Liu SH, Shu CM. Thermal parameters study of 1,1-bis(tert-butylperoxy)cyclohexane at low heating rates with differential scanning calorimetry. J Therm Anal Calorim. 2014;118:1675–83.
5. Cheng SY, Tseng JM, Lin SY, Gupta JP, Shu CM. Runaway reaction on tert-butyl peroxybenzoate by DSC test. J Therm Anal Calorim. 2008;93:121–6.
6. McIntosh RD, Waldram SP. Obtaining more, and better, information from simple ramped temperature screening tests. J Therm Anal Calorim. 2003;73:35–52.
7. Tsai YT, Cao CR, Chen WT, Chou WL, You ML. Using calorimetric approaches and thermal analysis technology to evaluate critical runaway parameters of azobisisobutyronitrile. J Therm Anal Calorim. 2015;122:1151–7.
8. Mathieu D. Significance of theoretical decomposition enthalpies for predicting thermal hazards. J Chem. 2015; Article ID 158794: 1:12.
9. Townsend I. Basic strategy for the thermal stability assessment of pharmaceutical synthetic intermediates and products. J Therm Anal Calorim. 1991;37:2031–66.
10. Anderson H, Mentel J. Adiabatic decomposition kinetics by nonlinear optimization. J Therm Anal Calorim. 1994;41:471–81.
11. Ende DJA, Ripin DHB, Weston NP. Thermal stability investigation of pyridine substituted tosyl oximes. Thermochim Acta. 2004;419:83–8.
12. Duh YS, Yo JM, Lee WL, Kao CS, Hsu JM. Thermal decompositions of dialkyl peroxides studied by DSC. J Therm Anal Calorim. 2014;118:339–47.
13. Lv JY, Chen WH, Chen YT, Yan JJ. Thermal risk evaluation on decomposition processes for four organic peroxides. Thermochim Acta. 2014;589:11–8.
14. Liu SH, Chen YC, Hou HY. Thermal runaway hazard studies for ABVN mixed with acids or alkalines by DSC, TAM III, and VSP2. J Therm Anal Calorim. 2015;122:1107–16.
15. Hou HY, Duh YS, Lin WH, Shu CM. Reactive incompatibility of cumene hydroperoxide mixed with alkaline solutions. J Therm Anal Calorim. 2006;85:145–50.
16. Kulkarni PB, Purandare GN, Nair JK, Talawar MB, Mukundan T, Asthana SN. Synthesis, characterization, thermolysis and performance evaluation studies on alkali metal salts of TABA and NTO. J Hazard Mater. 2005;119(53):61.
17. Carta A, Corona P, Loriga M. Quinoxaline 1,4-dioxide: a versatile scaffold endowed with manifold activities. Curr Med Chem. 2005;12:2259–72.
18. Vicente E, Villar R, Pérez-Silanes S, Aldana I, Goldman RC, Monge A. Quinoxaline 1,4-di-*N*-oxide and the potential for treating tuberculosis. Infect Dis Drug Targ. 2011;11:196–204.
19. Moreno E, Ancizu S, Perez-Silanes S, Torres E, Aldana I, Monge A. Synthesis and antimycobacterial activity of new quinoxaline-2-carboxamide 1,4-di-*N*-oxide derivatives. Eur J Med Chem. 2010;45:4418–26.
20. Ancizu S, Moreno E, Solano B, Villar R, Burguete A, Torres E, Perez-Silanes S, Aldana I, Monge A. New 3-methylquinoxaline-2-carboxamide 1,4-di-*N*-oxide derivatives as anti-Mycobacterium tuberculosis agents. Eur J Med Chem. 2010;18:2713–9.
21. Torres E, Moreno E, Ancizu S, Barea C, Galiano S, Aldana I, Monge A, Perez-Silanes S. New 1,4-di-*N*-oxide-quinoxaline-2-ylmethylene isonicotinic acid hydrazide derivatives as anti-Mycobacterium tuberculosis agents. Bioorg Med Chem Lett. 2011;221:3699–703.
22. Torres E, Moreno E, Galiano S, Devarapally G, Crawford PW, Azqueta A, Arbillaga L, Varela J, Birriel E, Di Maio R, Cerecetto H, Gonzalez M, Aldana I, Monge A, Perez-Silanes S. Novel quinoxaline 1,4-di-*N*-oxide derivatives as new potential anchagasic agents. Eur J Med Chem. 2013;66:324–34.
23. Millar RW, Philbin SP, Claridge RP, Hamid J. Studies of novel heterocyclic insensitive high explosive compounds: pyridines, pyrimidines, pyrazines and their bicyclic analogues. Propell Explos Pyrotech. 2004;29:81–91.
24. Tsai YT, Lin SY, Tong JW, Chen WC, Chen WT, Shu CM. Incompatible hazard investigation of a cycloaliphatic epoxy resin using green analytical method. J Therm Anal Calorim. 2015;122:1135–41.